CORE DESIGN FOR HETEROGENEOUS THORIUM FUEL ASSEMBLIES FOR PWR (II) - THERMAL HYDRAULIC ANALYSIS AND SPENT FUEL CHARACTERISTICS

KANG-MOK BAE[1], KYU-HYUN HAN[2], MYUNG-HYUN KIM[3*] and SOON-HEUNG CHANG[2]
[1]Currently with Korea Atomic Energy Research Institute
150 Deokjin-dong, Yuseong-gu, Daejeon 305-353, Korea
[2]Department of Nuclear and Quantum Engineering
Korea Advanced Institute of Science and Technology
373-1, Guseung-dong, Yuseong-gu, Daejeon 305-701, Korea
[3]Department of Nuclear Engineering, Kyung Hee University
YoungIn-shi, Gyeonggi-do, 449-701, Korea
*Corresponding author. E-mail : mhkim@khu.ac.kr

Received August 3, 2004
Accepted for Publication April 28, 2005

A heterogeneous thorium-based Kyung Hee Thorium Fuel (KTF) assembly design was assessed for application in the APR-1400 to study the feasibility of using thorium fuel in a conventional pressurized water reactor (PWR). Thermal hydraulic safety was examined for the thorium-based APR-1400 core, focusing on the Departure from Nucleate Boiling Ratio (DNBR) and Large Break Loss of Coolant Accident (LBLOCA) analysis. To satisfy the minimum DNBR (MDNBR) safety limit condition, MDNBR>1.3, a new grid design was adopted, that enabled grids in the seed and blanket assemblies to have different loss coefficients to the coolant flow. The fuel radius of the blanket was enlarged to increase the mass flow rate in the seed channel. Under transient conditions, the MDNBR values for the Beginning of Cycle (BOC), Middle of Cycle (MOC), and End of Cycle (EOC) were 1.367, 1.465, and 1.554, respectively, despite the high power tilt across the seed and blanket. Anticipated transient for the DNBR analysis were simulated at conditions of 112% over-power, 95% flow rate, and 2°C higher inlet temperature. The maximum peak cladding temperature (PCT) was 1,173K for the severe accident condition of the LBLOCA, while the limit condition was 1,477K. The proliferation resistance potential of the thorium-based core was found to be much higher than that of the conventional UO_2 fuel core, 25% larger in Bare Critical Mass (BCM), 60% larger in Spontaneous Neutron Source (SNS), and 155% larger in Thermal Generation (TG) rate; however, the radio-toxicity of the spent fuel was higher than that of UO_2 fuel, making it more environmentally unfriendly due to its high burnup rate.

KEYWORDS : Thorium Fuel Cycle, KTF, Proliferation Resistance, DNBR, LBLOCA

1. INTRODUCTION

Feasibility investigations into the use of heterogeneous thorium fuel in pressurized water reactors (PWRs) that are composed of seed and blanket regions, such as Radkowsky Thorium Fuel (RTF)[1], Whole Assembly Seed and Blanket (WASB)[2], and Kyung Hee Thorium Fuel (KTF) [3] reactors, have been performed by Ben-Gurion University, MIT, and Kyung Hee University, respectively. Optimization studies of the KTF design were conducted for fuel sizes, enrichments, and volume fractions of the seed and blanket to meet the design goals of an increasing fuel cycle economy and proliferation resistance. The optimized KTF assembly design concept was applied to the APR-1400 core and core analysis results showed compatible neutronic characteristics and a fuel cycle economy comparable to existing UO_2 PWR cores [4].

It is well known that ThO_2 has superior physical properties to UO_2 fuel, due to its high melting point, high thermal conductivity [5], and high stability at high burnup. In addition, U/Zr metal fuel has excellent physical properties, having both a high physical density and a high thermal conductivity. Although both characteristics are favorable as regards thermal hydraulic safety, a thorium-based core used with a KTF design requires advanced design modifications to ensure thermal hydraulic safety. For this case, some design approaches have been proposed to increase the DNBR margin, such as increasing the coolant mass flow rate in the seed channel, by using different grid loss coefficients, and increasing the fuel radius of the blanket.

This paper presents Part II of an investigation of a heterogeneous thorium fuel application for PWRs. In Part I [4], the optimization of the KTF assembly design and the neutronic characteristics of a core design with an optimized KTF assembly based on the APR-1400 conventional PWR were presented, and the fuel cycle economy was evaluated. In this paper, a thermal hydraulic safety analysis will be shown specifically for the thorium-based APR-1400 core, with thermal-hydraulic design limits of DNBR and LBLOCA. The spent fuel characteristics of proliferation resistance potential and fissile fraction limits were analyzed for the heterogeneous thorium fuel application core by use of bare critical mass (BCM), spontaneous neutron source rate (SNS), thermal generation rate (TG), plutonium production rate, and fissile fraction limit. Radio-toxicity was also calculated and compared to that of a conventional PWR to investigate the effects on the environment.

2. CHARACTERISTICS OF THE THORIUM-BASED ASSEMBLY AND CORE DESIGN

2.1 KTF Assembly Design Characteristics

The optimization of the KTF assembly design was performed with the goal of maximizing proliferation resistance and fuel cycle economy. The original KTF design was based on a seed-to-blanket ratio of 1:3 that had a penalty in fuel cycle economy and power peaking control. The pin peaking and fuel cycle economy of various seed-to-blanket ratios are shown in figure 1. It was considered that a large fraction of the seed assembly in the KTF design is favorable in terms of thermal hydraulic safety, though not in the fuel cycle economy. On the contrary, the small fraction of seed assembly in the KTF design is disadvantageous in terms of peaking control, but advantageous for fuel cycle economy. As seen in figure 1, a 1:1 ratio of seed-to-blanket in the KTF design provides optimal fuel cycle economy and thermal hydraulics safety. Therefore, the optimized KTF design has a 1:1 ratio of seed-to-blanket, although the parametric studies were performed based on a 1:3 ratio of seed-to-blanket, as presented in Part I of this paper [4].

In the KTF assembly, U/Zr, a metal alloy consisting of 10% zirconium and 90% of uranium, was used for a seed fuel, and a mixture of oxide fuel, containing 15 % of UO_2 mixed with 85% of ThO_2, was used as a blanket fuel. The enrichment of U-235 is 11 or 9 w% in the seed fuel and 12.5 w% in the blanket.

The U/Zr metallic fuel used as the seed fuel in the KTF design has inherent benefits compared to a UO_2 ceramic fuel, such as a higher physical density, a higher thermal conductivity, and a higher thermal heat capacity that can increase the thermal hydraulic safety margin. These are the main reasons why we used U/Zr metallic fuel for the seed. Normally, the linear heat rate of the seed fuel is higher than that of the blanket fuel, and the difference of linear heat rate between the seed and the blanket becomes larger when fresh seed fuel is loaded. Therefore, the thermal hydraulic safety margin of the thorium-based APR-1400 core was expected to be less than that of a conventional PWR. To evaluate the thermal margin of a thorium-based APR-1400 core in the event of a transient, as well as during steady-state operations, thermal hydraulic safety factors such as MDNBR and PCT were investigated. The DNBR is generally used as criteria for fuel integrity. Though it differs according to critical heat flux (CHF) correlation data, the MDNBR of a typical PWR during transient operation conditions should be higher than 1.3. To have higher MDNBR than 1.3 on DNB analysis, the KTF assembly design was modified to focus on rebalancing the power distribution between the seed and blanket. Figure 2 shows MDNBRs at various seed and blanket radii.

As shown in figure 2, a blanket fuel rod size larger than the seed fuel rod size is beneficial for obtaining a DNBR

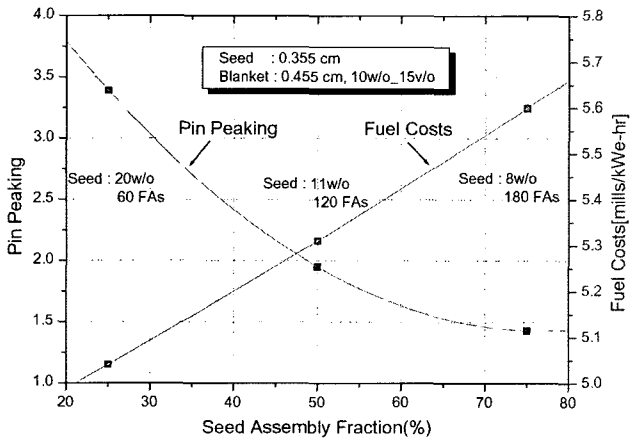

Fig. 1. Pin Peaking and Fuel Cycle Economics vs. Various Seed Assembly Fractions

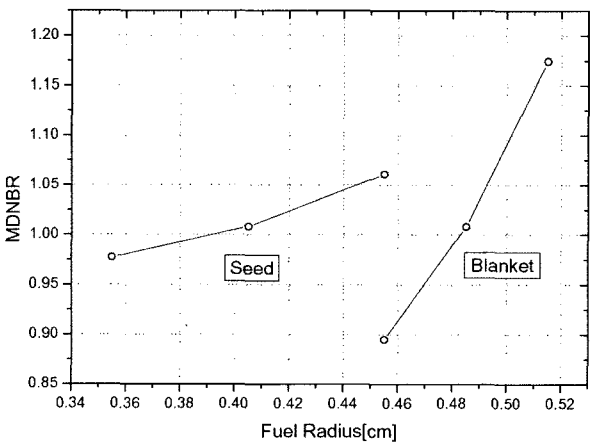

Fig. 2. MDNBR vs. Various Fuel Rod Sizes of Seed and Blanket

margin. This advantage is due to the different power generation rates between the seed and blanket. When the fuel surface area is enlarged by an increase of the fuel rod size, the DNBR will be changed to a positive direction for the fuel rod size. In addition, the enlarged blanket fuel rod size will increase the mass flow rate at a given seed channel, which might also positively effect the MDNBR. Therefore, the seed fuel should have a wider mass flow area than average PWR fuel in the sub-channel, so as not to breach the thermal hydraulic safety limit. However, even when a large blanket fuel rod size, 0.505cm, was used in the KTF color-set, the DNBR safety limit could not be satisfied.

New grid designs having different loss coefficients were suggested in order to solve the DNB problem as another way of increasing the thermal hydraulic safety margin. Grid loss coefficients as defined by Eq. (1) can be controlled by mechanical design separately at seed assembly and blanket assembly. Therefore, the grid loss coefficient was assumed to be small in the seed and large in the blanket to rebalance the mass flow rate at both regions, resulting in a higher flow rate in the seed and a lower flow rate in the blanket. The calculated MDNBR is presented in figure 3 with various seed and blanket grid loss coefficients. As can be seen in figure 3, the MDNBR fluctuates as the blanket loss coefficient is increased, because the increase raises the DNBR of the seed and lessens that of the blanket. Up to a blanket loss coefficient of 1.7, the MDNBR is high when the seed's loss coefficient is low, but if a blanket's loss coefficient is higher than 1.7, then the MDNBR is high when the seed's loss coefficient is high. This is because when a blanket loss coefficient is increased, the coolant flow is redirected to the seed region; hence, the MDNBR increases. However, the limiting rod size changes from the seed pin to the blanket pin when the blanket loss coefficient is increased to more than 1.7, as tradeoff occurs between the flow and heat flux in regard to the DNBR. As a result, the optimal loss coefficients were found to be 0.5 and 1.7 for the seed and the blanket, respectively, where as 0.5 of grid loss coefficient is used for the standard APR-1400 fuel design, on the assumption that new grid design with a high loss coefficient is possible. However, an increased loss coefficient in the blanket will increase the pressure drop by spacer grids, resulting in the need for increased pumping head for the reactor coolant pump.

$$\Delta P_K = K\frac{G^2}{2g\rho} \tag{1}$$

Where, G = axial mass flux,
g = gravitational acceleration, and
ρ = fluid density.

2.2 Thorium Based APR-1400 Core Characteristics

The proposed heterogeneous thorium-based APR-1400 core design concept was composed of a seed and blanket ratio of nearly 1:1. The APR-1400 thorium-based core had 468 EFPD fuel cycle lengths and 3983 MW thermal power generation with 241 fuel assemblies. All the parameters for thermal hydraulic safety analysis, except some geometry and fuel composition data of the fuel assembly, are identical to those of the APR-1400 UO_2 core. The thorium-based APR-1400 core has a different fuel cycle scheme between the seed and blanket. While the seed fuel assemblies have a three-batch reload scheme identical to the APR-1400 UO_2 fuel cycle, the blanket fuel assemblies are kept in the core for nine reload cycles as a single batch. Therefore, the thorium-based APR-1400 core has the advantage of a less spent fuel production rate, because the blanket fuel assemblies do not need to be entirely replaced until after nine reload cycles.

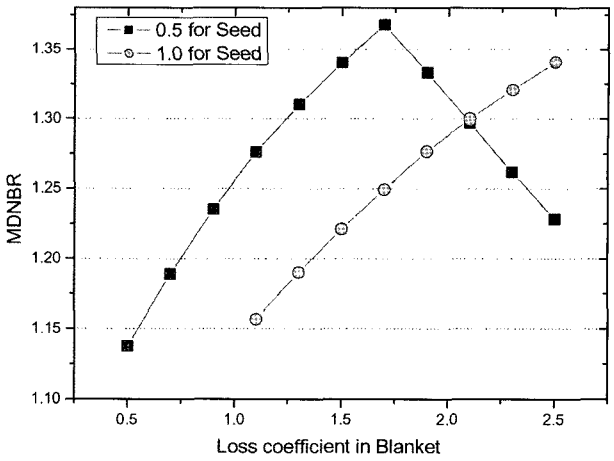

Fig. 3. MDNBR vs. Various Grid Loss Coefficients of Seed and Blanket

The maximum power peaking factor of the thorium-based APR-1400 core was 2.69 at Beginning Of Cycle (BOC), which exceeds the design limit value of the APR-1400 core. The design limit of the power peaking factor for the reference UO_2 core, APR-1400 is reported as 2.58. Therefore, a detailed examination is needed to ensure the fuel integrity of the KTF core, and the LBLOCA condition is considered.

2.3 Calculation Tools

The MATRA code was used to evaluate the DNBR analyses for the KTF core [6]. A hottest color-set geometry was selected as a sub-channel analysis model with power distribution data. A CE-1 correlation was used to calculate the CHF. Generally, a MDNBR limit is 1.13 in case of using the CE-1 correlation factor for a CHF calculation, however, 1.3 was recommended as a limit condition of MDNBR comprising uncertainty. For the LBLOCA analysis, the Multi-dimensional Analysis of Reactor Safety

(MARS) code was utilized. The MARS code was developed by KAERI to be used for multi-dimensional and multi-purpose optimal thermal hydraulic system analyses in PWR transients [7,8]. It was developed by integrating and restructuring RELAP5/MOD3.2.1.2 and COBRA-TF. These two codes were adopted to utilize the very general and versatile features of RELAP5 and the optimal 3-dimensional hydrodynamic module of COBRA-TF. The ORIGEN-II code was used to calculate the radio-toxicity of the spent fuel [9].

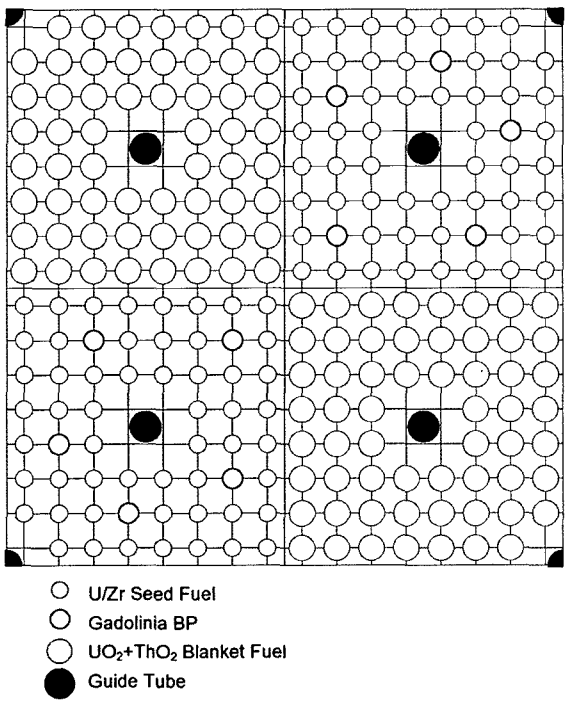

Fig. 4. Color-set Analysis Model of Sub-channels in KTF Core

3. THERMAL HYDRAULIC SAFETY ANALYSIS

3.1 DNBR Model Descriptions

Figure 4 shows the color-set model of the seed and blanket assembly used in the DNBR multi-channel analysis. As shown in figure 4, the modeling region consists of two quarters of seeds and two quarters of blankets. Because of

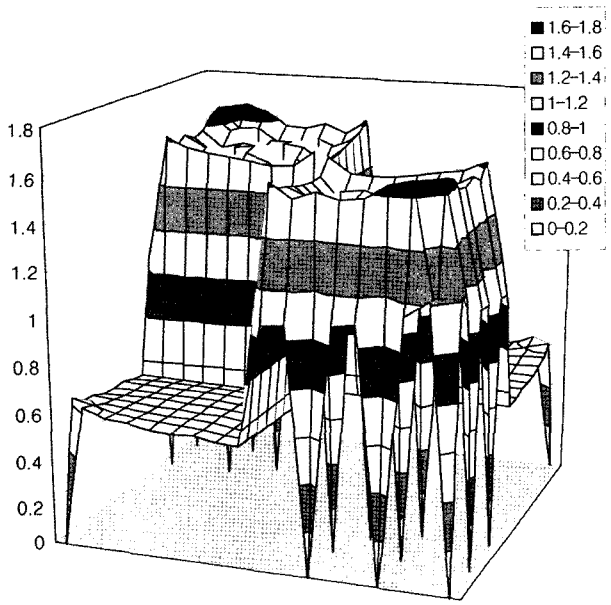

Fig. 5. Normalized Color-set Power Distribution

Table 1. Design Parameters of Seed and Blanket Assembly

Parameter	Optimized Assembly Design	
	Seed	Blanket
Pellet Radius (cm)	0.325	0.4395
Gas Gap (cm)	-	0.0085
Cladding Thickness (cm)	0.03	0.057
Fuel Rod Radius (cm)	0.355	0.505
Number of Fuel Rods	236 fuel rods 5 guide tubes	236 fuel rods 5 guide tubes
Fuel Cell Pitch (cm)	1.285	1.285
Assembly Gap (cm)	0.218	0.218
Fuel Assembly Width (cm)	20.56	20.56

Table 2. Parameters of MATRA Code for DNBR Analysis

Reactor power	100% power (3983MWth)
Inlet Temperature	291 °C
Whole core coolant flow rate	20.36 Mg/sec
Local loss coefficient of grids	0.5 (seed), 1.7 (blanket)
Axial power profile	given as a table
Axial friction coefficient (turbulent)	$0.184*Re^{-0.2}$
Turbulent mixing model	Equal mass exchange
Cross-flow convergence limit	0.1
CHF correlation	CE-1 (D_{hy} = 22.51 mm for seed pin, 10.71 mm for blanket pin)

Table 3. Calculated MDNBR of Steady State Analysis

Seed diameter	BOC		MOC		EOC	
	Using AECL Lookup table	Using CE-1 correlation	Using AECL Lookup table	Using CE-1 correlation	Using AECL Lookup table	Using CE-1 correlation
7.1 mm	1.807	1.665*	1.970	1.839*	1.947	1.861*
7.6 mm	1.860	1.715	-	-	-	-
9.6 mm	1.917	1.766	2.084	1.945	2.064	1.974

* : Predicted value based on the DNBR data calculated using AECL Lookup table

the color-set geometry, the analysis was done with attention paid to the spacer grid effects on the pressure drop in the borderline between the two different assemblies. The design parameters of the color-set model for DNBR analysis are shown in table 1. Because of the different channel geometries between the seed and the blanket, the coolant speeds differ from each other, and the cross flow is a vital factor in DNBR analysis. For the pin power distribution, an assembly-wise pin power distribution was multiplied with maximum relative assembly power ratios, which were 1.125, 1.139, and 1.096 for the BOC, MOC, and EOC, respectively. The normalized pin power distribution used in the three cases, BOC, MOC, and EOC, is shown in figure 5.

A minimum DNBR was observed in the seed assembly because of high pin power, even with a larger coolant flow. However, the fuel pin with the highest pin power does not always exhibit minimum DNBR in the core. Table 2 shows the major thermal hydraulic parameters of the MATRA analysis model.

3.1.1 Steady-state Analysis

A steady-state analysis was conducted based on the conditions given in Table 2. As the core of APR-1400 was a CE design core, CHF calculation was performed using a CE-1 correlation. However, the CE-1 correlation was known to be applicable only for a geometry with a fuel pin diameter from 7.63 mm to 9.7 mm. Because the diameter of the seed pin in the KTF, 7.1 mm, is smaller than a conventional PWR fuel pin, we cannot evaluate the DNBR directly using MATRA. A DNBR analysis with MATRA for seed pins of radius 7.1 mm, 7.6 mm, and 9.6 mm using the AECL lookup table is shown in Table 3. A fitting curve derived from above calculation was applied to the calculation results of two cases (for seed pins of radius 7.6 mm and 9.6 mm) from MATRA using CE-1 correlations. From this fitting method, the MDNBRs at BOC, MOC, and EOC were predicted to be 1.582, 1.781, and 1.882 - all higher than 1.3. The MDNBR under operational transient conditions was evaluated for the BOC condition, where the lowest value is obtained under the steady-state.

3.1.2 DNBR Transient Analysis

First, a DNBR analysis was done without applying the new grid loss coefficient, i.e., for an assembly design with standard spacer grids. For a transient analysis of the

DNBR limit, the overpower transient was assumed identical to that of an MIT approach. The condition that the inlet coolant temperature is increased by 2°C, the coolant flow is reduced by 5%, and the reactor power is increased to 112% was used by MIT for a thermal hydraulic analysis of the WASB design [10]. The limiting case, BOC, was analyzed and the MDNBR was calculated to be 1.137, which did not satisfy the design limit goal of 1.3.

To solve the DNBR problem, the new grid design was applied, as described in Section 2.1. New grids in the blanket assembly will increase the grid loss coefficient from 0.5 to 1.7, will increase the pressure drop, and will increase the coolant mass flow into the hot seed fuel regions. Using this grid design, the DNBR analysis was repeated with a limited condition that total coolant flow rate remained unchanged, even with an increased pressure drop. The MDNBR was 1.367, which was slightly higher than the design goal.

Figure 6 shows the MDNBR variation along the axial length. The MDNBRs of the BOC, MOC, and EOC are 1.367, 1.465, and 1.554, respectively, all of which are higher than the 1.3 limit condition. The axial position where the MDNBR occurs is higher for the EOC and lower for the BOC. Figure 7 shows a coolant temperature change in the hottest sub-channel. Because the boiling temperature at 15.5MPa is 345°C, boiling doesn't occur at the exit for all three cases. The coolant exit temperature is higher in the MOC, and lower in the EOC. Figure 8 shows the coolant exit enthalpy distribution of the BOC. It was observed that the gadolinia rod flattens enthalpy distribution nearby. Due to the biased flow toward the seed region, enthalpies in the blanket region are higher.

3.2 LBLOCA Simulation

3.2.1 Geometry Modeling

A LBLOCA is considered one of the most serious types of accidents that can occur in water-cooled reactors. In an LBLOCA, the major concern is the PCT limit to prevent a catastrophic accident resulting in a core meltdown. In this study, a thermal hydraulic analysis of the LBLOCA using MARS was performed. To analyze the transient condition, a steady-state calculation should be carried out preliminary to understand system operation and to obtain design parameters. For the analysis of transients in a

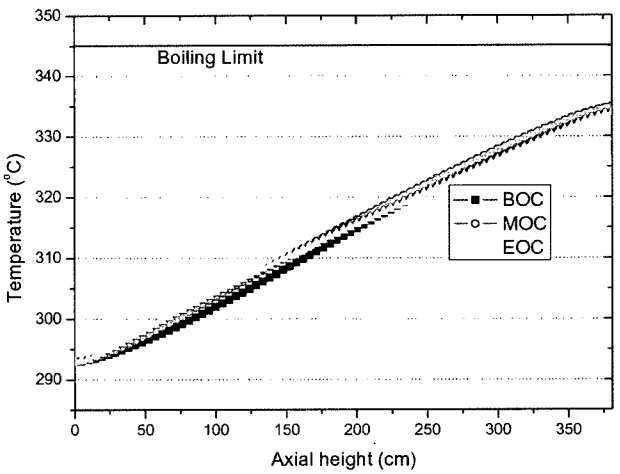

Fig. 7. Coolant Temperature Variations in the Hottest Seed Sub-Channel

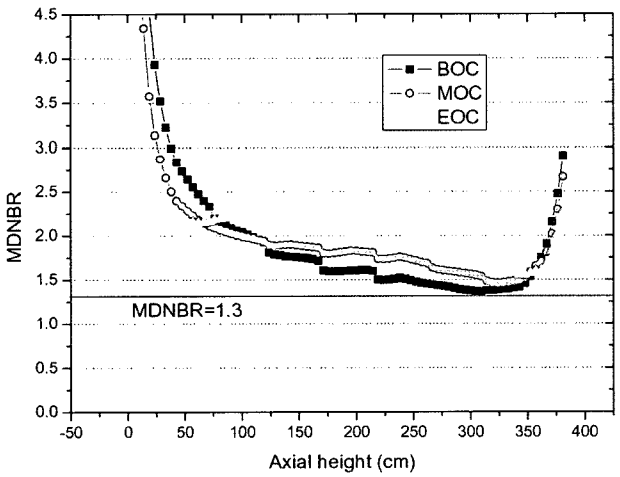

Fig. 6. MDNBR of the Hottest Seed Sub-Channel at BOC, MOC and EOC

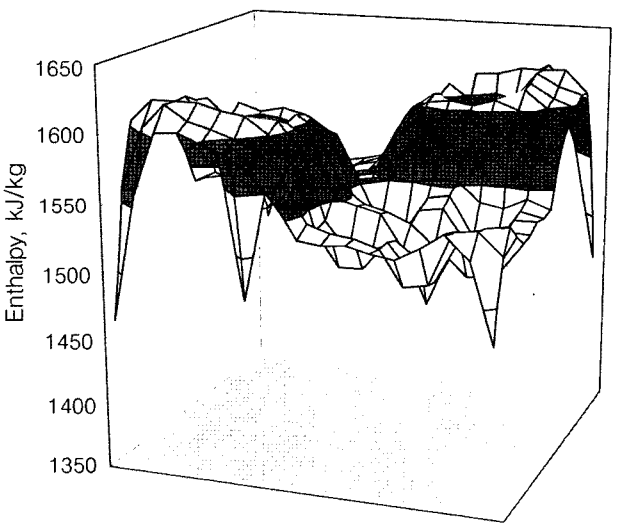

Fig. 8. . Exit Enthalpy Distribution in the Hottest Coolant Channel at BOC

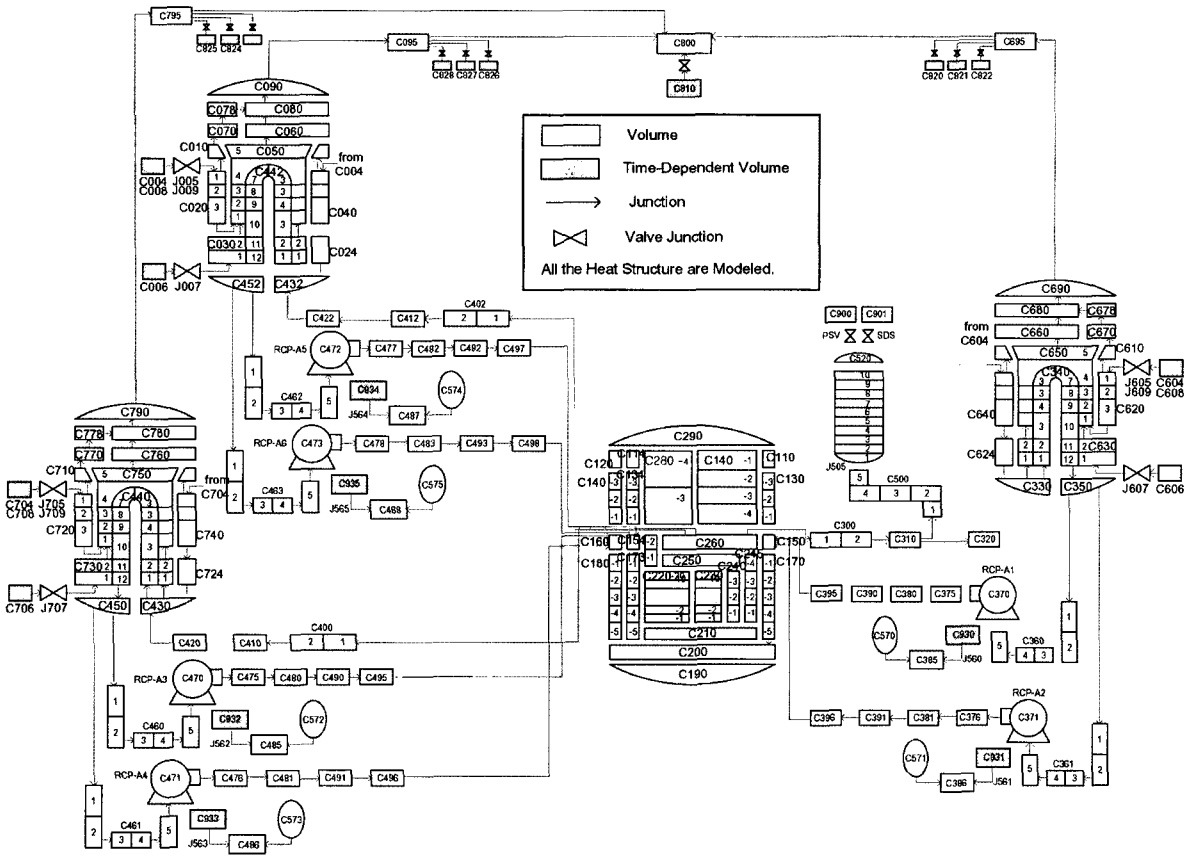

Fig. 9. System Modeling of Thorium Based APR-1400 Core for MARS

Table 4. KTF Core Design Parameters for LBLOCA Simulation

Parameters	Models
Initial Power	102% of 3983 MWth
Transient Power	
- Kinetics and Trip Reactivity	conservative
Core & Fuel Modeling	
- # of Axial Nodes	20
- Core Flow Channels	Average (240 FAs) and Hot (1 FA)
- Total Pin Peaking	1.914
• Axial Power Distribution	given as a table
• Assembly-wise Peaking	1.123
• Pin Peaking in Color-set (seed and blanket)	1.704 (embedded in hot channel)
- Gap Conductance	Constant

thorium-based APR-1400 core, the LBLOCA input deck of the reference APR-1400 UO_2 core was modified. The system modeling of the APR-1400 is shown in figure 9.

The fuel geometries, power distributions, and material properties of metal U/Zr and $(Th+U)O_2$ were changed to reflect the new core design. In the core model, two flow paths were used considering cross-flow. The average core flow path depicted an average heat output of 240 assemblies and the other single flow path represented the highest heat output assembly. To obtain the required initial condition, a steady-state calculation was done. The LOCA calculation began with flow, temperature, heat output, and steady-state pressure prior to the assumed break. Once the parameters of fluid temperature, flow pressure, loop pressure drop, and fuel rod coincided with the input parameters and an acceptable steady-state was achieved, MARS was ready to calculate the LOCA transients. Important parameters of the core and fuel modeling are shown in Table 4.

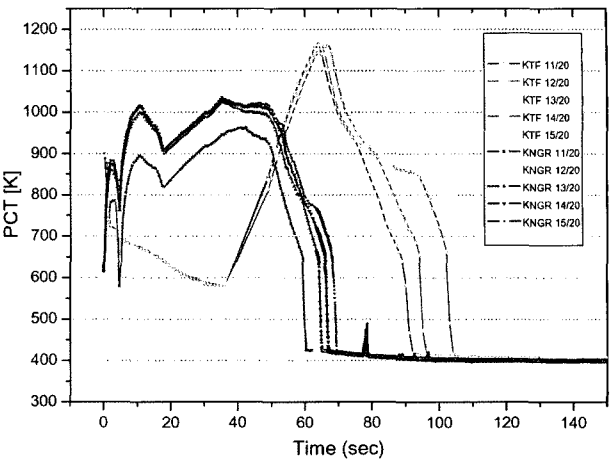

Fig. 11. Peak Cladding Temperature at the Hottest Fuel Rod

3.2.2 LBLOCA Analysis Results

The LOCA analysis was performed using a Korean version of RELAP, MARS in a conservative approach. The initial reactor power was assumed to be 102% of nominal level. For the LBLOCA calculation, we assumed a double-ended guillotine cold leg break. There are four High Pressure Safety Injection (HPSI) pumps in the APR-1400 system. After a 35-second delay from the reactor trip signal, only two of four pumps can be operated and two of them are regarded as having failed to consider single active failure for the LBLOCA accident. The discharge coefficient was considered as 1.0. A pressurizer was isolated to prevent the injection of non-condensable gas into the primary system in the event of a decrease of the pressure level of less than 0.1 m; the minimum safety injection tank coolant capacity was assumed, and no fluidic device was present. The minimum high pressure safety injection flow rate was 100%. The ANS73 decay model was applied. However, the axial power distribution used in the MATRA had 24 nodes, while MARS had 20 nodes, which required transformation. Major parameters for both the KTF and the APR-1400, such as the down-comer flow path, the condensed level, and the fuel cladding temperature, were compared.

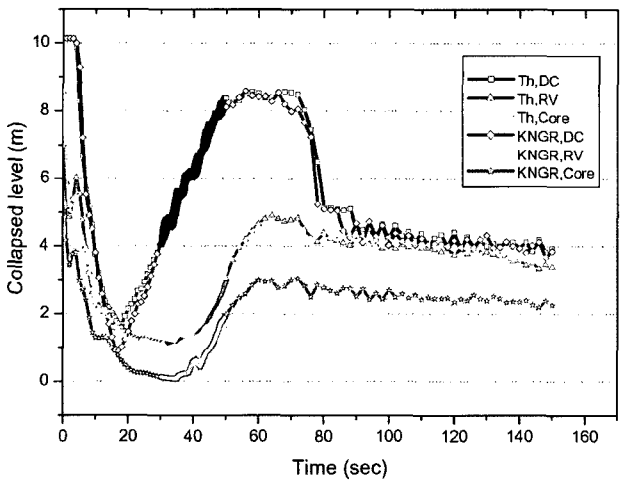

Fig. 10. Condensed Level Variations in Down-comer, Reactor Vessel and Core

Anticipated important accidents were as follows. As the LBLOCA was initiated and blow-down progressed, the core heat output decreased abruptly and the primary system pressure decreased. The blow-down was initially reduced abruptly and fluctuated due to the safety injection. The core was evacuated at 35 seconds, and the coolant level increased until the core was reflooded. When the low plenum was reflooded, the down-comer level increased, because the safety injection flows through the down-comer. The core condensed level increases continuously and reaches half the height of the core. Figure 10 shows the condensed levels of the down-comer, vessel, and core. The fuel cladding is not rewetted as the down-comer condensed level is reduced to slightly lower than the cold leg, and the core condensed level is maintained at 2/3rd of core height. Due to the initial blow-down, The fuel cladding temperature rose abruptly.

After evacuating the safety injection tank, the reduced safety injection water partially condensed into steam in the loop, and the down-comer was nearly saturated by the heat that was transferred. The peak cladding temperature, as illustrated in figure 11, shows the differences between the KTF and the APR-1400. As predicted, an acute blow-down peak (727K) is observed, and a gradual reflood

peak (973K) is seen afterwards. The peak cladding temperature of the KTF is 1,173 K, which is lower than the limiting temperature of 1,477 K. Note that the benefits obtained from utilizing the U/Zr fuel in reducing the PCT could also be realized if U/Zr fuel were used in the APR-1400 UO_2 core.

4. CHARACTERISTICS OF SPENT FUEL

4.1 Proliferation Resistance

Increased proliferation resistance potential is one of the main advantages of using a thorium-based fuel. Usually,

Table 5. Nuclear Properties of Fissile and Fertile Nuclear Materials [10]

ISOTOPE	Critical Mass*(kg)	Spontaneous Neutron Source Neutrons/sec-kg	Thermal Generation Rate Watts/kg
Pu-238	10	2.67E6	560
Pu-239	10.2	21.8	2.0
Pu-240	36.8	1.03E6	7.0
Pu-241	12.9	49.3	6.4
Pu-242	89	1.73E6	0.12

Table 6. Isotope Weight Fraction in the Discharged Spent Fuel Assembly

ISOTOPE	APR-1400*	KTF Seed **	KTF Blanket***
Th-232	-	-	78.3139
U-233	-	-	1.4621
U-234	-	-	0.3856
U-235	0.8292	0.6593	0.1732
U-236	0.6066	1.4060	0.2707
U-238	91.9133	85.4333	11.2665
Np-237	0.0752	0.1509	0.0443
Np-239	0.0093	0.0089	0.0028
Pu-238	0.0343	0.0968	0.0334
Pu-239	0.6145	0.4855	0.1578
Pu-240	0.2696	0.3047	0.0613
Pu-241	0.1837	0.1750	0.0611
Pu-242	0.0832	0.1583	0.0631
Am-241	0.0061	0.0066	0.0022
Am-243	0.0217	0.0484	0.0340
Am-242m	0.0001	0.0001	0.0
Cm-242	0.0024	0.0038	0.0013
Cm-244	0.0095	0.0343	0.0220

* : B_d = 52.0 MWd/kgHM ** : B_d = 83.0 MWd/kgHM *** : B_d = 96.0 MWd/kgHM

Table 7. Measured Proliferation Resistance Indices

ISOTOPE	APR-1400	KTF		
		Seed	Blanket	Average
BCM (kg)	22.19	27.44	28.15	27.83
SNS (#/kg-sec)	4.33E5	6.93E5	6.94E5	6.94E5
TG (Watts/kg)	19.83	47.90	52.69	50.54

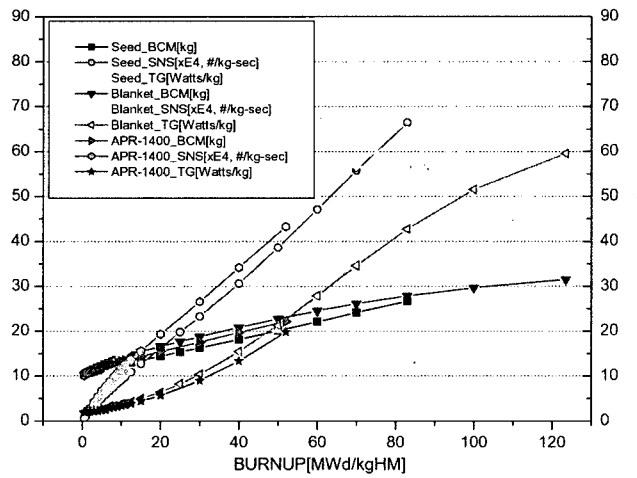

Fig. 12. Proliferation Resistance Indices vs. Burnup

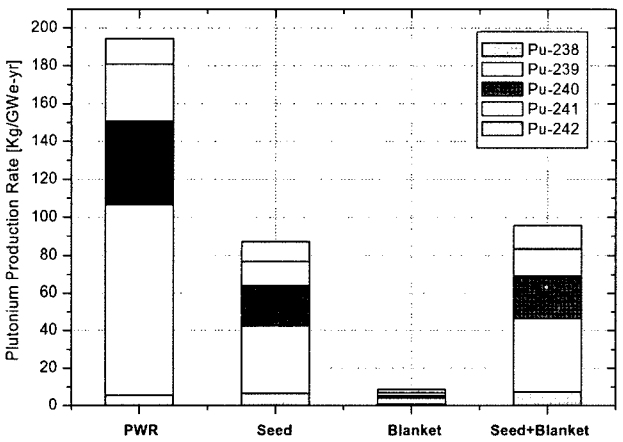

Fig. 13. Plutonium Production Rates

the proliferation resistance of a fuel cycle depends upon the quantity and quality of the plutonium isotopes in the discharged spent fuel. A larger fraction of fertile isotopes in a plutonium nuclide can generate both a large amount of decay radiation and the spontaneous neutron source that provide an intrinsic barrier against reaching critical mass for a nuclear weapon. The proliferation resistances were described by BCM, SNS, and TG indices which were obtained by using the plutonium isotope weight fraction in spent fuel, as shown in table 5. Table 6 shows the isotope weight percentage in the discharged seed and blanket.

As can be seen in the results presented in table 7, a thorium-based core has a higher proliferation resistance potential by having larger indices by 25% in BCM, by 60% in SNS and by 155% in TG, than that of the APR-1400 UO_2 fuel core. The blanket assembly has better proliferation resistance than the seed assembly, because of the high burnup of the spent fuel. Figure 12 represents the BCM, SNS, and TG values at each burnup point. It can be seen that the discharged fuel burnup is significant for increasing the proliferation resistance of the spent fuel. If a fuel is taken to as high discharge burnup as the blanket fuel, similar improved proliferation resistance can be obtained from the APR-1400 UO_2 or other PWR designs.

The BCM, SNS, and TG indices can assume the qualitative analysis method because they depend only upon the fraction of plutonium isotopes. There is another way to assess proliferation resistance potential based on the quantitative analysis method, by comparing the plutonium amount at the discharged burnup point. For this reason, plutonium production rates were investigated, and these rates are presented in figure 13. The total plutonium production rate of the heterogeneous thorium-based fuel core is much lower than that of the reference UO_2 core. The annual production rate of plutonium from a thorium-based core is decreased by 46% compared with the reference UO_2 core, due to the use of a single batch fuel scheme for blanket fuel assembly during the nine seed cycles.

4.2 Fissile Uranium Isotope Limit

In a thorium-fueled core, U-233 converted from Th-232 is one of the major fissile isotopes. As far as the threat of proliferation is concerned, an acceptable concentration of fissile uranium content among the total uranium is reported as to be less than 12 w/o [11]. This content is nearly equi-

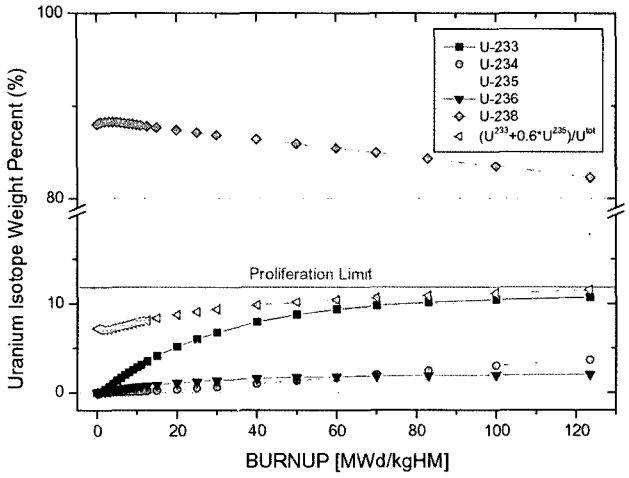

Fig. 14. Uranium Isotopes Fraction Variations vs. Burnup

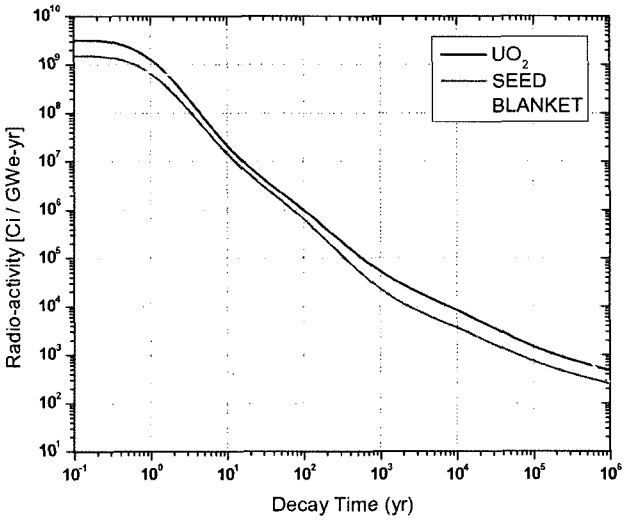

Fig. 15. Radio-activity of Spent Fuel vs. Decay Time

valent to the 20 w/o of U-235 in a conventional uranium-oxide fuel core. The uranium isotope content of the blanket assembly in the KTF core is shown in figure 14. The uranium fissile fraction does not reach the limit condition during a 120 MWd/kgHM burnup; therefore, there is no threat of fissile uranium content proliferation.

4.3 Radio-Toxicity of Spent Fuel

The radio-toxicity of the KTF spent fuel was analyzed by using the ORIGEN-II code, and the results are presented in figure 15. The radioactivity of the blanket is higher than that of UO_2 or seed assembly due to the high burnup, because the blanket assemblies remain in the core for up to nine seed cycles. In the blanket assembly, Th-228, decayed from Th-232 via alpha and beta decay, gradually decays into Ra-224, then Rn-220, and then Po-216, through its decay chain series. Each nuclide maintains a secular equilibrium state between daughter nuclei. For this reason, high radioactivity can remain for 100 years in the blanket assembly. There is a hump of radioactivity of the blanket assembly between 10,000 and 1 million years, because of the decay product of U-233. The radio-toxicity of the seed assembly is slightly higher than that of conventional UO_2 fuel, and so the KTF design is disadvantageous from an environmental standpoint.

5. CONCLUSIONS

A KTF assembly design using a heterogeneous seed and blanket concept was applied to the APR-1400 core to determine its feasibility of use in a PWR. In this paper, a thermal hydraulic safety analysis was conducted for the thorium based APR-1400 core. It was shown that a thorium-based core could be maintained within LBLOCA accident safety limits, as well as within the operational transient conditions of DNBR. A thorium-based core also offers better proliferation resistance potential as regards BCM, SNS, and TG indices. However, it was found to be less environmentally friendly than UO_2 fuel, because of the high radio-toxicity of the spent fuel involved, on the contray, high radioactivity can provide a barrier to approach. Therefore, the heterogeneous seed and blanket concept of the KTF design for a PWR application was found to have neutronic feasibility, as well as an advantageous fuel cycle economics, satisfying the thermal hydraulics safety limits.

REFERENCES

[1] A. Galperin, E. Shwageraus and M. Todosow, "Thorium Fuel cycles for Light Water Reactors: Homogeneous Design," *Trans. Am. Nucl. Soc.*, **83**, November (2000).

[2] D. Wang, M. J. Driscoll and M. S. Kazimi, "Design and Performance Assessment of a PWR Whole-Assembly Seed and Blanket Thorium Based Fuel cycle," MIT-NFC-TR-026, MIT Nuclear Engineering Department, September (2000).

[3] K.H. Kim, K.M. Bae and M.H. Kim, "Optimization of Thorium-Based Seed and Blanket Fuel Assembly Design for PWR," Trans. Am. Nucl. Soc., Vol.86, pp. 302-303, June (2002).

[4] K.M. Bae and M.H. Kim, "Core Design for Heterogeneous Thorium Fuel Assemblies for PWR(I)-Nuclear Design and Fuel Cycle Economy," *Nuclear Engineering and Technology*, **37**, 91 (2005).

[5] B.M. Ma, "Nuclear Reactor Materials and Application," Van Nostrand Reinhold Company Inc. (1983).

[6] Y.J.Yoo and D.H. Hwang, "Development of a sub-channel Analysis Code MATRA," KAERI/TR-1033/98 (1998).

[7] W.J. Lee et al., "Development of a multi-dimensional realistic thermal-hydraulic system analysis code, MARS 1.3 and its verification," KAERI/TR-1108/98 (1998).

[8] RELAP5-3D Code Manual Volume 1: Code Structure, System Models and Solution Methods, INEEL-EXT-98-00834, Revision 2.2, October (2003).
[9] A. G. Croff, "A User's Manual for the ORIGEN-2 Computer Code," ORNL TM-7175, Oak Ridge National Laboratory, July (1980).
[10] D. Wang, "Optimization of Seed and Blanket Thorium-Uranium Fuel Cycle for Pressurized Water Reactors," Ph. D. Thesis, MIT (2003).
[11] C.W. Forsberg, C.M. Hopper and H.C.Vantine, "What is Nonweapons-Usable U-233?" *Trans. Am. Nucl. Soc.*, **81**, November (1999).